

Analytical Methods

Accepted Manuscript



This is an *Accepted Manuscript*, which has been through the Royal Society of Chemistry peer review process and has been accepted for publication.

Accepted Manuscripts are published online shortly after acceptance, before technical editing, formatting and proof reading. Using this free service, authors can make their results available to the community, in citable form, before we publish the edited article. We will replace this *Accepted Manuscript* with the edited and formatted *Advance Article* as soon as it is available.

You can find more information about *Accepted Manuscripts* in the [Information for Authors](#).

Please note that technical editing may introduce minor changes to the text and/or graphics, which may alter content. The journal's standard [Terms & Conditions](#) and the [Ethical guidelines](#) still apply. In no event shall the Royal Society of Chemistry be held responsible for any errors or omissions in this *Accepted Manuscript* or any consequences arising from the use of any information it contains.



Journal Name

ARTICLE

Electrochemical immunoassay based on polythionine as signal source for the sensitive detection of carcinoma embryonic antigen

Received 00th January 20xx,

Min Chen^{a,*}, Chengfei Zhao^{b,1}, Qingshan Xu^c, Biqiong Nie^d, Liufang Xu^d, Shaohuang Weng^{e,*} and Xinhua Lin^e

Accepted 00th January 20xx

DOI: 10.1039/x0xx00000x

www.rsc.org/

In this work, an effective immunosensor based on polythionine (PTH) as signal source was fabricated for the facile and sensitive detection of carcinoma embryonic antigen (CEA) in human serum. With the help of nafion, anti-CEA antibodies were immobilized on the surface of PTH modified electrode. The morphology and electrochemical behaviors of the fabrication process of the immunosensor were characterized with electrochemical impedance spectroscopy (EIS), differential pulse voltammetry (DPV) and atomic force microscopy (AFM), respectively. The rangeability of anodic peak current before and after the CEA immobilization was directly related to the concentration of CEA. A linear equation of the CEA concentration range from 1×10^{-12} to 1×10^{-6} $\text{g} \cdot \text{mL}^{-1}$ with a detection limit of $0.1 \text{ pg} \cdot \text{mL}^{-1}$ was obtained. The proposed method had high sensitivity, good selectivity and acceptable reproducibility for the detection of CEA. The analytical results of serum specimen show that the proposed immunosensor has a promising alternative approach for the detection of biomarkers in the clinical diagnosis.

1. Introduction

An ideal biomarker, which is responsible for clinical diagnosis, would clearly distinguish between normal and diseased states, especially for the initial stage of serious diseases. Facile and accurate detection of tumor marker plays a crucial role in clinical diagnosis, therapy and research of cancer [1]. Carcinoma embryonic antigen (CEA) is a 180 kDa oncofetal protein and a well-known tumor-associated marker [2], belonging to the family of cell surface glycoprotein [3]. The normal range of CEA levels is less than $2.5 \text{ ng} \cdot \text{mL}^{-1}$ in an adult non-smoker and $5.0 \text{ ng} \cdot \text{mL}^{-1}$ in a smoker [4]. However, the increase level of CEA exists in about 95% of colon tumors [5] and 38.6% of breast cancer [6]. Furthermore, CEA is associated with ovarian carcinoma [7], lung cancer [8] and gastric cancer [9]. The variable levels of CEA in serum or other biofluids are close related to the occurrence and progression of tumors. Hence, it can be directly used for evaluating curative effect and

judging recrudescence or metastasis of cancers, especially for the early stage of cancer [10]. Thus, development of a special, sensitive and easy control assay for CEA is very important.

Up to now, a number of immunoassay methods for CEA, including chemiluminescence immunoassay [11], enzyme-linked immunosorbent assay [12], fluoroimmunoassay [13] and electrochemical immuno-assay [14], have been reported. However, these methods are somewhat limited to the disadvantages, such as time-consuming, qualified personnel and sophisticated instrumentation. Therefore, development of an easy-control method with high sensitivity and specificity for the facile detection of CEA is still highly desired. Compared with primary methods, electrochemical immunoassays have recently attracted much interest because of their advantages of easy operation, simple instruments, excellent sensitivity and selectivity [15-16]. As an important kind of electrochemical immunoassays, label-free electrochemical immunosensors developed for measuring biomarkers with the variable responses have attracted widespread interests [17-18]. In the design and fabrication of electrochemical label-free immunosensor, signal generation and amplification is the crucial step. In this perspective, nanomaterials containing electrochemical redox mediators, such as prussian blue [19], $\text{K}_3[\text{Fe}(\text{CN})_6]$ [20] and toluidine blue [21] have been adopted and used to fabricate electroactive interfaces for label-free electrochemical biosensor. Recently, the preparation of polythionine (PTH) from the aromatic rings of thionine (Th) linked together via -NH- bridges in suitable situation had attracted increasing attention. As a kind of electrode material, PTH exhibits fast charge transfer capacity with great potential for bioanalytical applications [22-24]. Up to now, PTH and its

^a Department of Orthopedic Surgery, Affiliated Union Hospital of Fujian Medical University, Fuzhou 350001, China.

^b Pharmaceutical and Medical Technology College of Putian University, Putian 351100, China.

^c Department of Orthopedic Surgery, Affiliated Mindong Hospital of Fujian Medical University, Ningde 355000, China.

^d School of Basic Medical Sciences, Fujian Medical University, Fuzhou 350108, China.

^e Department of Pharmaceutical Analysis, Faculty of Pharmacy, the higher educational key laboratory for Nano Biomedical Technology of Fujian Province, Fujian Medical University, Fuzhou 350108, China.

* Corresponding author: shweng@fjmu.edu.cn (S. H. Weng), Tel./fax: +86 591 22862016, chenminfz006@163.com (M. Chen); Tel./fax: +86 591 83357896.

1: Min Chen and Chengfei Zhao contributed equally to this work.

Electronic Supplementary Information (ESI) available: [Characterization of the prepared steps of immunosensor by AFM; Comparison of analytical performances for CEA and the real application]. See DOI: 10.1039/x0xx00000x

composites have been widely used for building biosensors in measuring glucose [23], dopamine [25], biomarkers [26] and DNA [24, 27]. Although, some applications in electrochemical sensor based on PTh [26] or thionine [28] have been developed, reported applications in electrochemical immunosensor with excellent analytical performance remain inchoate, and the obstacles mainly originate from the preparation of PTh with sensitive electrochemical response towards the variance of modified electrode.

In this work, a simple, but effective electrochemical strategy based on polythionine (PTh) as signal substance for ultrasensitive detection of CEA was developed. PTh was synthesized through a one-pot synthesis method in aqueous solution. The synthetic process of PTh has the advantages of non-toxic chemical reagent and simple synthetic steps. In addition, the PTh modifying GCE generated outstanding and impressible electrochemical signals in neutral solution. What's important, the electrochemical signals of PTh changed sensitively with different layers that modified on the surface of GCE. Thus, according to the characteristic, the PTh was used to modify GCE to prepare an electrochemical label-free immunosensor for the detection of CEA, as shown in Fig.1. The prepared PTh was dropped on the GCE to form the signal indicator layer. After the cover of nafion, antibody can strongly fix on the surface of nafion via electrostatic or physical interactions to be the complete immunosensor. When incubated with CEA, the formation of the immunocomplex towards CEA through immunoreactions will reduce the current response of the constructed full electrochemical loop containing signal indicator layer due to the non-conductive property of CEA [20]. As for the sensitively changed effect of PTh, the decreased electrochemical response before and after the formation of immunocomplex can be used to quantify the concentration of CEA.

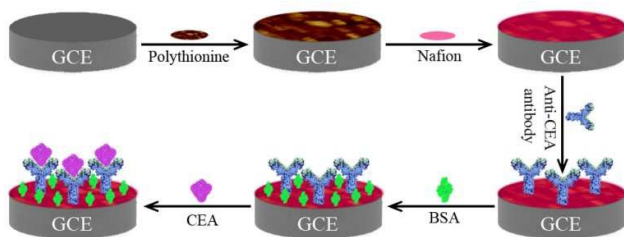


Fig. 1. Schematic diagram of the proposed method for CEA detection.

2. Experimental

2.1 Reagents and apparatus.

CEA antibody (Anti-CEA) and CEA standard solutions were purchased from Zhengzhou Biocell Biotechnology Co., Ltd (Zhengzhou, China). Bovine serum albumin (BSA, 99%), Thionine acetate salt and nafion (~5% in a mixture of lower aliphatic alcohols and water) were purchased from Sigma. N,N-dimethylformamide (DMF), HCl, HNO₃, ethanol, K₃[Fe(CN)₆], K₄[Fe(CN)₆]•3H₂O, Na₂HPO₄•12H₂O, KH₂PO₄, FeCl₃•6H₂O, NaCl,

KCl, NaOH, Tween-20 and H₂O₂ were obtained from Sinopharm Chemical Reagent Co., Ltd. All of the reagents were used directly.

Phosphate Buffer Saline (PBS) was prepared with 0.1 g KH₂PO₄, 1.45 g Na₂HPO₄•12H₂O, 0.1 g KCl and 4 g NaCl in 500 ml ultrapure water and the pH was adjusted to be 7.0 with HCl or NaOH. The PBS was used as the solution of diluting anti-CEA and antigen, and the electrolyte of detection. The washing buffer was that PBS mixed with 0.05% (w/v) Tween-20. Ultrapure water (resistivity >18.2 MΩ•cm) purified through a Millipore water purification system was used throughout the experiments.

The measurements of electrochemical impedance spectroscopy (EIS) and differential pulse voltammetry (DPV) were carried out at Autolab PGSTAT302F system (Eco Chemie, The Netherlands) in a solution containing 10 mmol/L [Fe(CN)₆]^{3-/4-} and 1 mol•L⁻¹ KCl and CHI 660C electrochemical workstation (Shanghai ChenHua Instruments Co., China) in PBS (pH=7.0), respectively. A conventional three-electrode system containing a modified glass carbon electrode (GCE, Φ=3 mm) as the working electrode, a platinum electrode as the counter electrode, and Ag/AgCl electrode as the reference electrode was employed for the electrochemical detection. The detailed parameters of all DPVs were as follows: initial potential was -0.5 V; final potential was 0.3 V; increment was 0.004 V; amplitude was 0.05 V; pulse width was 0.05 s; sample width was 0.0167 s; pulse period was 0.2 s; quiet time was 2 s; and sensitivity was 10⁻⁵ A/V.

2.2 Preparation of polythionine (PTh)

Polythionine was facilely synthesized according to the reported literature with some modification [18]. 0.05 g FeCl₃ was dissolved in 50 ml deionized water with vigorous stirring. After that, 0.1 g thionine was added into the FeCl₃ solution at 50 °C, and then 2 ml 30% H₂O₂ was added. After 24 h reaction, the black material was collected by centrifuging at 3000 rpm for 30 min and then was repeatedly washed respectively three times with 0.1 mol•L⁻¹ HCl and deionized water to remove impurities. The obtained polymer was dried in vacuum at 40 °C for 24 h. 5 mg prepared polythionine (PTh) was dissolved in 5 mL DMF and sonicated for 30 min to obtain PTh suspension with dark-blue color.

2.3 Fabrication of electrochemical immunosensor

Before surface modification, the GCE was respectively polished with alumina powder of 1.0, 0.3 and 0.05 μm on microcloth pad and then cleaned ultrasonically in HNO₃ solution (volume ratio of HNO₃ to water is 1:1), ethanol and deionized H₂O, respectively. 3 μL of PTh suspension was dropped on the cleaned GCE and dried at room temperature for 24 h to obtain PTh/GCE. Then, 3 μL of 1% nafion dropped onto PTh/GCE and dried at room temperature for 60 min to form nafion/PTh/GCE. Next, 6 μL of 80 μg•mL⁻¹ anti-CEA was immobilized on the surface of nafion/PTh/GCE with the condition of 37 °C and 60% humidity for 2h, the modified electrode was thoroughly washed with PBST, PBS and deionized water in turn to remove the nonspecific adsorption of anti-CEA. After that, the modified electrode was blocked in 1% BSA solution for 60 min to obtain Ab/nafion/PTh/GCE, namely electrochemical

immunosensor. At last, the Ab/nafion/PTH/GCE was washed several times with PBST, PBS and deionized water for the assay measurement. The prepared Ab/nafion/PTH/GCE was stored at 4 °C when not in use.

2.4 Electrochemical measurements of CEA

6 μ L of different concentrations of the CEA were respectively dropped on the Ab/nafion/PTH/GCE at 37 °C for 60 min to form immunocomplex by immunoreaction. After carefully washed, the formed electrode, named as Ag/Ab/nafion/PTH/GCE, was measured by DPV in PBS. The current signal changes of modified electrode before and after the immunoreaction were used for the determination of CEA.

3. Results and discussion

3.1 Characterization of PTH

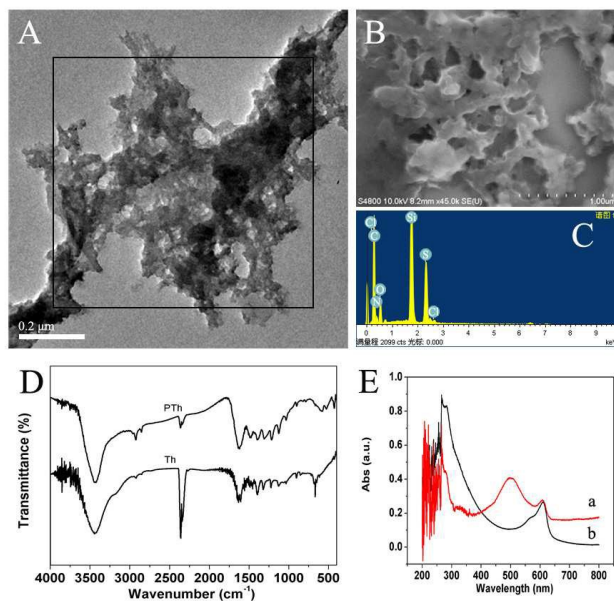


Fig. 2. TEM (A), SEM (B) image and EDS (C) characteristics of PTH, the compared FTIR spectra (D) of PTH and thionine, and the UV-vis spectra (E) of thionine (a) and PTH (b) in DMF.

As shown in Fig. 2A, the TEM image of the PTH indicated that the morphology of PTH contains nano-network structure composed of relatively uniform fibers and particles. The fibers with tens nanometers widths and particles form an ordered nanostructure. Furthermore, the high magnification SEM image shown in Fig. 2B further reveals that the fibrous and granular PTH can form a uniform and even partially tight film on solid surface. Additionally, the chemical composition of PTH was determined using the energy-dispersed spectrum (EDS) in the SEM system, as shown in Fig. 2C. The peaks of C, S, N and Cl are observed, indicating that PTH is from thionine with the FeCl_3 co-oxidation. FTIR and UV-vis spectra were further applied to discuss the molecular structure of PTH, as shown in Fig. 2D, E. Besides the similar infrared absorption of PTH and monomer in the range of 600 cm^{-1} to 2000 cm^{-1} , the two more strong bands of PTH at 2921 cm^{-1} and 2851 cm^{-1} indicate that

the aromatic C–H stretching vibration of PTH when the polymerization of thionine happened [25, 29]. Additionally, the enhanced band at about 3500 cm^{-1} assigned to the N–H stretching vibration of the amino moieties also indicates the formation of polythionine. Furthermore, Fig. 2E shows the absorption spectrum of PTH in DMF. The strong absorption peak at 283 nm, red shift compared with thionine monomer, is assigned to the transition of phenothiazine ring. Moreover, the red shift of absorption peak in the visible light region at 612 nm compared with thionine suggests the strengthened conjugation degree of PTH in the polymerization process [28].

3.2 Characterization of the prepared step of immunosensor

The step-by-step modified processes of the prepared immunosensor were characterized by AFM technique, as shown in Fig. S1. Fig. S1A is the AFM image of bare GCE, showing intrinsic morphology of GCE with clear shallow graben rille. AFM image (Fig. S1B) depicts that PTH modified GCE composed of well distribution of large amounts of uniform flakiness or films, which are consistent with the result of SEM. The prepared nafion/PTH/GCE showed a compact, homogeneous and porous film, as shown in Fig. S1C. Herein, the covered nafion with porous and uniform structure can be an effective entrapment medium for the assembly of anti-CEA [30]. Furthermore, AFM image in Fig. S1D exhibited that a noteworthy aggregation of the trapped biomolecules with hundreds nanometer size was formed due to the immobilization of protein [31], indicating that anti-CEA successfully and largely bound on nafion/PTH/GCE to fabricate Ab/nafion/PTH/GCE [18]. The results of perspective morphology illustrates the proposed immunosensor could be successfully prepared step by step.

3.3 Electrochemical monitoring of different modified electrodes

EIS was used to characterize the modification process of GCE to verify the fabrication process of the immunosensor. Fig. 3A shows the Nyquist plots of stepwise modification of the prepared immunosensor, and the insert is an equivalent circuit of modified electrode. The electron-transfer resistance (R_{et}) is reflected by the semicircle diameter of the Nyquist plot, which controls the electron transfer kinetics of $[\text{Fe}(\text{CN})_6]^{4-/3-}$ between the modified electrode surface and the solution. The Nyquist plot of bare GCE (curve a) is an almost straight line, estimating the R_{et} equaled to zero. When modified with PTH (curve b), the R_{et} increases significantly to be about $1000\ \Omega$, implying that the modified PTH on the surface GCE hinders the transfer of $[\text{Fe}(\text{CN})_6]^{4-/3-}$. After nafion covered PTH/GCE (curve c), the R_{et} further increases to about $1500\ \Omega$, indicating the successful immobilization of nafion [18]. With the continue immobilization of anti-CEA on nafion/PTH/GCE (curve d), the R_{et} further enlarges to about $2100\ \Omega$, meaning that the antibodies successfully fasten onto the surface of nafion and the non-conductive protein molecules prevent the transfer of $[\text{Fe}(\text{CN})_6]^{4-/3-}$. With the blocking of BSA, the R_{et} of the blocked electrode (curve e) further increases ($3000\ \Omega$). At last, after the immobilization of CEA on the electrode through immunoreaction, the R_{et} of CEA/BSA/antibody/nafion/PTH/GCE (curve f) enlarges to $4000\ \Omega$, indicating the immunocomplex formed and the

concentration of CEA could be detected by the prepared electrode facily.

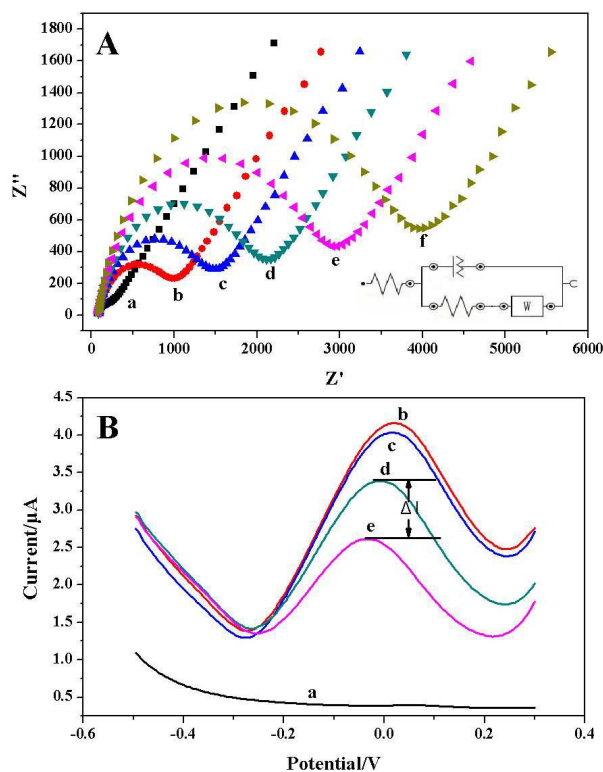


Fig. 3. (A) Nyquist plots of EIS of bare GCE (curve a), PTh/GCE (curve b), nafion/PTh/GCE (curve c), antibody/nafion/PTh/GCE (curve d), BSA/antibody/nafion/PTh/GCE (curve e) and CEA/BSA/antibody/nafion/PTh/GCE (curve f); insert was an equivalent circuit of EIS; (B) DPV curves of bare GCE (curve a), PTh/GCE (curve b), nafion/PTh/GCE (curve c), BSA/antibody/nafion/PTh/GCE (curve d) and CEA/BSA/antibody/nafion/PTh/GCE (curve e).

In the meantime, we investigated DPV of different steps of the immunosensor, as shown in Fig. 3B. DPV of bare GCE (curve a) is almost straight line and no redox peak found. After modified with PTh, an obvious well-defined anodic peak appears at about 0.03 V (curve b), implying PTh can easily adhere to the electrode surface and produce obvious response. When nafion covered the PTh/GCE, the DPV anodic peak is a little low (curve c) due to the resistance and charge hindrance of pure nafion, suggesting that the adjustment of the surface of PTh/GCE could make the electrochemical response sensitively change. The anodic response of PTh gradually decreases with the process of immobilization of anti-CEA and BSA (curve d). The key advantage of nafion illustrates the ability to fix proteins containing antibody on the electrode surface strongly through electrostatic or physical interactions and blocks interferences in clinical serum with high specificity [18, 30]. When CEA combined with antibody on the immunosensor by immunoreaction, the anodic peak current value of

CEA/BSA/antibody/nafion/PTh/GCE (curve e) dramatically decreases. In such testing system, modified electrode, electrolyte and counter electrode forms a full electrochemical loop containing PTh layer [20]. The immobilization of insulative CEA will inhibit the electron transfer in the total electrochemical loop to reduce the current response [19-20, 26]. Thus, the reduced current amplitude before and after the immobilization of CEA (ΔI) can be used to quantify the concentration of CEA accurately and facily.

3.4 Quantitative detection of CEA

The proposed immunosensor was further employed to detect CEA quantitatively through DPV, as shown in Fig. 4. The decrease amplitude of the DPV peak current of the electrode (ΔI) increases gradually with CEA concentration varied in the range from $1 \times 10^{-12} \text{ g} \cdot \text{mL}^{-1}$ ($1 \text{ pg} \cdot \text{mL}^{-1}$) to $1 \times 10^{-6} \text{ g} \cdot \text{mL}^{-1}$ ($1 \text{ } \mu\text{g} \cdot \text{mL}^{-1}$), as shown in the insert of Fig. 4. The variable quantity of DPV peak current is acceptably proportional to the logarithm of CEA concentration, which revealed a good linear relationship. The corresponding calibration curve is shown in Fig. 4. The linear equation is $\Delta I (\mu\text{A}) = 3.0687 + 0.2049 \log C_{\text{CEA}} (\text{g} \cdot \text{mL}^{-1})$, and the square of correlation coefficient (R^2) is 0.9953. The limit of detection (LOD) was calculated to be $0.1 \text{ pg} \cdot \text{mL}^{-1}$, based on $3\sigma/\text{slope}$ (σ represents the standard deviation of the blank values ($n=9$) and slope represents the slope of calibration curve). It is observed that the proposed immunoassay had low LOD and broad linear range towards CEA (Table 1). As shown in the comparable results of several electrochemical immunosensor for CEA in Table 1, both of LOD and linear range of the proposed method are excellent. The excellent performance of this method for CEA might be attributed to the outstanding electrochemical response of the prepared PTh. Additionally, the relative standard deviation (RSD) values of the tested ΔI of different concentrations of CEA were 1.4%, 3.8% and 4.5% for 10^{-11} , 10^{-9} and $10^{-7} \text{ g} \cdot \text{mL}^{-1}$ of CEA, respectively, indicating the excellent reproducibility of the constructed immunosensor. On the basis of the low LOD, wide linear range and outstanding reliability, the proposed immunosensor can favorably determinate the different concentrations of CEA.

3.5 Specificity of the immunosensor

The specificity of electrochemical biosensor plays a significant role in biological test without complicated separation. Several common proteins which coexisted in clinical system might disturb the signal response of the prepared immunosensor. Thus, the selectivity of the proposed immunosensor was evaluated towards some common interfering proteins, including AFP, PSA, CA125, CA153 and CA19-9. Compared with the variable quantity of response current of the proposed immunosensor under the same condition in PBS and $1 \text{ ng} \cdot \text{mL}^{-1}$ CEA, the decrements of current are close to the blank value when AFP, PSA, CA-125, CA-153, and CA-199 were detected. As shown in Fig. 5A, the results of the common interfering proteins are much smaller, suggesting that these interferences did not give rise to a remarkable current shift or current change. At the same time, when $1 \text{ ng} \cdot \text{mL}^{-1}$ of CEA mixed with AFP, PSA, CA-125, CA-153, or CA19-9, the different variable quantities of DPV peak current were also measured, as shown

in the Fig. 5B. Compared with the response of simple CEA, the current variations of different interference protein are less than 8.9%, indicating that the common interference could not impact the immunosensor for CEA assay. Thus, the results imply that the proposed immunosensor possesses excellent specificity for CEA.

Table 1 Comparison of analytical performances of several label-free electrochemical immunosensors for CEA

| Sensors | Signal source | Linear range ($\text{g}\cdot\text{ml}^{-1}$) | LOD ($\text{fg}\cdot\text{ml}^{-1}$) | Reference |
|---------------------------------------------------|------------------------------------|-------------------------------------------------------------------|-------------------------------------------|-----------|
| anti-CEA/ AgNPs-THI-ICP fibres | $[\text{Fe}(\text{CN})_6]^{4-/3-}$ | 5×10^{-14} - 10^{-12} and 10^{-12} - 10^{-7} | 0.5 | 32 |
| anti-CEA/ Graphene-Au-THI nanocomposites | Thionine | 10^{-11} - 3.0×10^{-7} | 650 | 33 |
| anti-CEA/Ag-SiO ₂ @nafion/THI@CHIT/GCE | Thionine | 10^{-15} - 10^{-10} | 1 | 34 |
| anti-CEA/PEI/AuNP@nafion/FC@CHIT/GCE | $[\text{Fe}(\text{CN})_6]^{3-}$ | 10^{-11} - 1.5×10^{-7} | 300 | 35 |
| anti-CEA/Au/ ferricyanide-doped polyaniline/GCE | $[\text{Fe}(\text{CN})_6]^{3-}$ | 10^{-12} - 5.0×10^{-7} | 100 | 14 |
| anti-CEA/Au/PATP/GCE | $[\text{Fe}(\text{CN})_6]^{4-/3-}$ | 10^{-15} - 10^{-8} | 0.015 | 36 |
| anti-CEA/AuNPs-GP-CS/Ag/Au electrode | $[\text{Fe}(\text{CN})_6]^{4-/3-}$ | 10^{-14} - 10^{-9} | 5.0 | 37 |
| Anti-CEA/nafion/PTh | polythionine | 10^{-12} - 10^{-6} | 100 | This work |

3.6 Practical application of the proposed immunosensor

In order to evaluate the actual application potential of the proposed immunosensor, CEA was firstly detected in the fetal calf serum samples through the standard addition method. The experimental results were summarized in Table S1, that the recoveries of CEA showed an acceptable values from 93.4 % to 98.4%, indicating that the proposed immunosensor owned the possibility of clinical application. Besides, we applied the prepared immunosensor to directly determinate the human serum samples to investigate the reliability of the proposed method. Two CEA levels were selected, one is less than $5.0 \text{ ng}\cdot\text{mL}^{-1}$ as negative control samples, and the other is higher than $5.0 \text{ ng}\cdot\text{mL}^{-1}$ as positive samples [4-6]. Compared with the results of chemiluminescent immunoassay, Table S2 show that the measured values of the proposed immunosensor are close to that of chemiluminescent immunoassay with the absolute value of relative errors of the two methods less than 6%. Therefore, the results suggest that the proposed immunoassay has the great application potential in clinical diagnostics for accurate determination of CEA.

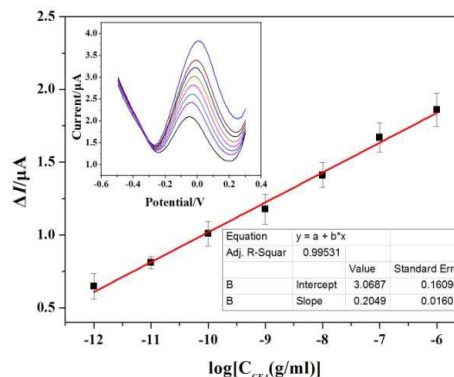


Fig. 4. Calibration plots of anodic peak current versus logarithm of CEA concentration, error bars represent the SDs from three independent detections; the insert shows the DPV curves of the prepared immunosensor upon the immersion into different concentrations of CEA.

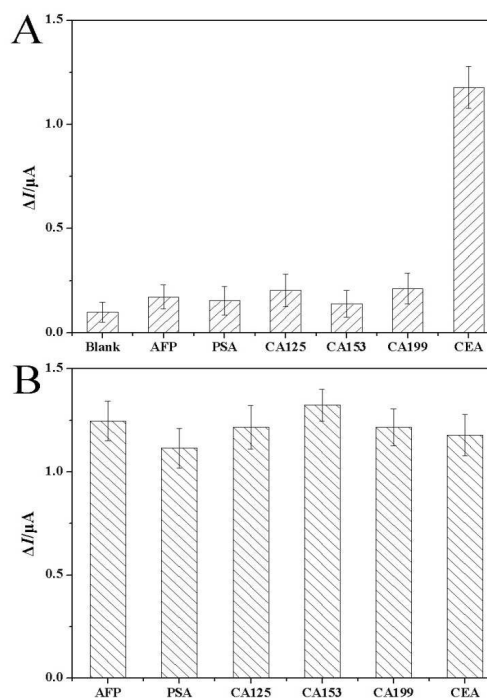


Fig. 5. (A) The anodic peak current of the prepared immunosensor to blank liquid, AFP ($1 \text{ ng}\cdot\text{mL}^{-1}$), PSA ($1 \text{ ng}\cdot\text{mL}^{-1}$), CA-125 ($1 \text{ IU}\cdot\text{mL}^{-1}$), CA-153 ($1 \text{ IU}\cdot\text{mL}^{-1}$), CA-199 ($1 \text{ IU}\cdot\text{mL}^{-1}$) and CEA ($1 \text{ ng}\cdot\text{mL}^{-1}$); (B) The anodic peak current of the prepared immunosensor to CEA ($1 \text{ ng}\cdot\text{mL}^{-1}$) + AFP ($1 \text{ ng}\cdot\text{mL}^{-1}$), CEA ($1 \text{ ng}\cdot\text{mL}^{-1}$) + PSA ($1 \text{ ng}\cdot\text{mL}^{-1}$), CEA ($1 \text{ ng}\cdot\text{mL}^{-1}$) + CA-125 ($1 \text{ IU}\cdot\text{mL}^{-1}$), CEA ($1 \text{ ng}\cdot\text{mL}^{-1}$) + CA-153 ($1 \text{ IU}\cdot\text{mL}^{-1}$), CEA ($1 \text{ ng}\cdot\text{mL}^{-1}$) + CA-199 ($1 \text{ IU}\cdot\text{mL}^{-1}$) and CEA ($1 \text{ ng}\cdot\text{mL}^{-1}$). The error bars represent the SDs from three independent detections.

Conclusions

In this paper, we reported a simple and reliable amperometric immunosensor based on a nafion/PTH modified GCE for the precise and sensitive detection of CEA. The advantages of prepared immunosensor are as follows: the proposed strategy provided a simple and convenient method to fabricate the immunosensor and had acceptable performance for the response for CEA; nafion with excellent biocompatibility was used to stabilize electrochemical signal and bound adequate amount of anti-CEA antibody on the modified electrode. The response of the prepared immunosensor had a good linear relation with CEA concentration from 1×10^{-12} to 1×10^{-6} $\text{g} \cdot \text{mL}^{-1}$ with a $0.1 \text{ pg} \cdot \text{mL}^{-1}$ of LOD. Meanwhile, the immunosensor was applied to determinate CEA levels in the human serum samples, the results of which were satisfactory, comparing with that of chemiluminescent immunoassay. On the basis of the above reasons, the electrochemical immunosensor can be an excellent candidate method for the clinical application.

Acknowledgements

This work is supported from the National Science Foundation of Fujian Province (2015J01475, 2015J01043), the Medical Elite Cultivation Program of Fujian Province (2013-ZQN-JC-16), the Science and technology project of the Education Department of Fujian Province (JA15445), and the Innovation and Entrepreneurship Training Programs for College Students of Fujian Province (201410392048).

Notes and references

#Footnotes relating to the main text should appear here. These might include comments relevant to but not central to the matter under discussion, limited experimental and spectral data, and crystallographic data.

- 1 D. Faraggi, Kramar, *Urol Oncol-Semin Ori.*, 2000, 5, 211.
- 2 T. Ojima, M. Iwahashi, M. Nakamura, K. Matsuda, M. Nakamori, K. Ueda, T. Naka, K. Ishida, F.J. Primus, H. Yamaue, *Int. J. Cancer*, 2006, 120, 585.
- 3 S. Hammarström, *Semin. Cancer Biol.*, 1999, 9, 67.
- 4 M. J. Goldstein, E.P. Mitchell, *Cancer Invest.*, 2005, 23, 338.
- 5 J.P. Tiernan, S.L. Perry, E.T. Verghese, N.P. West, S. Yeluri, D. G. Jayne, T.A. Hughes, *Brit. J. Cancer*, 2013, 108, 662.
- 6 A. C. Pedersen, P. D. Sørensen, E. H. Jacobsen, J. S. Madsen, I. Brandslund, *Clin. Chem. Lab. Med.*, 2013, 51, 1511.
- 7 MJA. Engelen, HWA. de Bruijn, H. Hollema, K. A. ten Hoor, PHB. Willemse, J. G. Aalders, van der Zee AGJ, *Gynecol. Oncol.*, 2000, 78, 16.
- 8 L. Hernández, A. Espasa, C. Fernández, A. Candela, C. Martín, S. Romero, *Lung Cancer*, 2002, 36, 83.
- 9 S. Ishigami, S. Natsugoe, S. Hokita, X.M. Che, K. Tokuda, A. Nakajo, H. Iwashige, M. Tokushige, T. Watanabe, S. Takao, T. Aikou, *J. Clin. Gastroenterol.*, 2001, 32, 41.
- 10 Á. Szilvás, A. Blázovics, G. Székely, E. Dinya, J. Fehér, G. Mózsik, *J. Physiol-Paris*, 2001, 95, 247.
- 11 J. C. Forest, J. Masse, A. Lane, *Clin. Biochem.*, 1998, 31, 81.
- 12 L. S. Zhao, S. Y. Xu, G. Fjaertoft, K. Pauksen, L. Håkansson, P. Venge, *J. Immunol. Methods*, 2004, 293, 207.
- 13 F. Yan, J. N. Zhou, J. H. Lin, H. X. Ju, X. Y. Hu, *J. Immunol. Methods*, 2005, 305, 120.
- 14 S. J. He, Q. Y. Wang, Y. Y. Yu, Q. J. Shi, L. Zhang, Z. G. Chen, *Biosens. Bioelec.*, 2015, 68, 462.

- 15 J. Wu, Z. F. Fu, F. Yan, H. X. Ju, *Trends Anal. Chem.*, 2007, 26, 679.
- 16 Y. Wan, Y. Su, X. H. Zhu, G. Liu, C. H. Fan, *Biosens. Bioelec.*, 2013, 47, 1.
- 17 S. C. B. Gopinath, Thean-Hock Tang, M. Citartan, Y. Chen, T. LakshmiPriya, *Biosens. Bioelec.*, 2014, 57, 292.
- 18 S. H. Weng, M. Chen, C. F. Zhao, A. L. Liu, L. Q. Lin, Q. C. Liu, J. H. Lin, X. H. Lin, *Sens. Actua. B.*, 2013, 184, 1.
- 19 F. Y. Kong, B. Y. Xu, Y. Du, J. J. Xu, H. Y. Chen, *Chem. Commun.*, 2013, 49, 1052.
- 20 M. Chen, C. F. Zhao, W. Chen, S. H. Weng, A. L. Liu, Q. C. Liu, Z. F. Zheng, J. H. Lin, X. H. Lin, *Analyst*, 2013, 138, 7341.
- 21 H. P. Peng, Y. Hu, P. Liu, Y. N. Deng, P. Wang, W. Chen, A. L. Liu, Y. Z. Chen, X. H. Lin, *Sens. Actua. B.*, 2015, 207, 269.
- 22 Y. Liu, H. L. Zhang, G. S. Lai, A. M. Yu, Y. M. Huang, D. Y. Han, *Electroanalysis*, 2010, 22, 1725.
- 23 W. W. Tang, L. Li, L. J. Wu, J. M. Gong, X. P. Zeng, *Plos One*, 2014, 9, e95030.
- 24 N. Zhang, K. Y. Zhang, L. Zhang, H. Y. Wang, H. W. Shi, C. Wang, *Anal. Methods*, 2015, 7, 3164.
- 25 C. F. Zhao, Z. Q. Jiang, X. H. Cai, L. Q. Lin, X. H. Lin, S. H. Weng, *J. Electroanal. Chem.*, 2015, 748, 16.
- 26 S. H. Weng, Q. C. Liu, C. F. Zhao, G. L. Hong, Z. Q. Jiang, L. Q. Lin, Y. Chen, X. H. Lin, *Sensors Actuator B*, 2015, 216, 307.
- 27 H. Y. Huang, W. Q. Bai, C. X. Dong, R. Guo, Z. H. Liu, *Biosens. Bioelec.*, 2015, 68, 442.
- 28 H. P. Peng, Y. Hu, A. L. Liu, W. Chen, X. H. Lin, X. B. Yu, *J. Electroanal. Chem.*, 2014, 712, 89.
- 29 Y. Kong, S. L. Mu, *Acta Phys. Chim. Sin.*, 2001, 17, 295.
- 30 A. F. Chetcuti, D. K. Wong, M. C. Stuart, *Anal. Chem.*, 1999, 71, 4088.
- 31 G. S. Lai, J. Wu, C. Leng, H. X. Ju and F. Yan, *Biosens. Bioelectron.*, 2011, 26, 3782.
- 32 W. B. Lu, X. W. Cao, T. Lin, J. Ge, J. Dong, W. P. Qian, *Biosens. Bioelec.*, 2014, 57, 219.
- 33 X. L. Jia, Z. M. Liu, N. Liu, Z. F. Ma, *Biosens. Bioelec.*, 2014, 53, 160.
- 34 R. X. Wang, X. Chen, J. Ma, Z. F. Ma, *Sens. Actua. B*, 2013, 176, 1044.
- 35 W. T. Shi, Z. F. Ma, *Biosens. Bioelec.*, 2011, 26, 3068.
- 36 Z. M. Liu, Z. F. Ma, *Biosens. Bioelec.*, 2013, 46, 1.
- 37 S. Saluma, N. Apon, L. Warakorn, K. Proespichaya, T. Panote, *Analytica Chimica Acta*, 2015, 853, 521.